Temperature Dependence of the Lattice Vibrations in ND_4Cl†

H. C. Teh and B. N. Brockhouse
Department of Physics, McMaster University, Hamilton, Ontario, Canada
(Received 28 March 1973)

Translational and librational modes in ND_4Cl at the high-symmetry points Γ, X, M, R in the Brillouin zone were studied over a temperature range from 82 to 300 °K by coherent inelastic scattering of thermal neutrons utilizing the McMaster triple-axis crystal spectrometer at Chalk River. The temperature dependence of the frequencies and widths were obtained from the measurements. Several modes were found to undergo an abrupt decrease in frequency in the vicinity of the order-disorder transition ($T_\lambda = 249.5$ °K), while others are insensitive to the transition. The widths of the neutron groups for some of the modes increased rapidly at temperatures beyond 200 °K. The dynamics of those lattice modes associated with the phase transition is briefly discussed. In addition some acoustic modes at small waves vectors were measured, and the associated elastic constants (c_{11} and c_{44}) calculated, as functions of temperature. An interesting effect was noted. The constant c_{11} as measured for ND_4Cl with neutrons (and thus appropriate to very high frequencies) shows much less effect of the transition than does c_{11} measured for NH_4Cl at ultrasonic frequencies. The effect is believed to arise from the kinetics of the ordering process.

I. INTRODUCTION

Complete dispersion curves[1] of ND_4Cl in the principal symmetry directions at 85 °K have been measured using coherent inelastic scattering of thermal neutrons. The experimental results were satisfactorily described by a many-parameter shell-model calculation.[2] Recently, additional model calculations[3,4,5] have been reported.

Of special interest is the λ transition in the ammonium halides. In the case of ND_4Cl the well-known transition at 249.5 °K is understood to be of order-disorder type[6] involving the reorientation of the ND_4^+ ion within the cubic unit cell. Extensive studies on the nature of the λ transition have been reported by many workers: the internal modes and the librational modes of the ammonium ions (in both the deuterated and nondeuterated ammonium bromide and chloride) have been measured[7] by infrared techniques. The external transverse-optical modes in the ammonium halides have been measured by far-infrared absorption and Raman scattering[8] from liquid-He to room temperature. Observations by optical harmonic scattering techniques[9] have revealed phenomena interpreted as coming from the presence of long-range order well above T_λ in NH_4Cl. The decay of short-range order below T_λ in NH_4Br has been observed by Raman techniques.[10] Measurements of the adiabatic elastic constants of NH_4Cl by ultrasonic techniques[11] have shown pronounced anomalous behavior in the vicinity of T_λ. Much higher frequency acoustic phonons (10^{11} to 10^{12} Hz) have been measured[12] in NH_4Cl by coherent inelastic neutron scattering. The derived elastic constants obtained by the two methods were found to be in substantial agreement within the comparatively large errors of the latter method, although some differences are visible.

In this paper we report detailed measurements of the translational and librational (torsional) modes in ND_4Cl at the high-symmetry points in the Brillouin zone over a temperature range from 82 to 300 °K. Some acoustic modes at small wave vectors and the associated elastic constants were also studied. The lattice dynamics associated with the phase transition is discussed on the basis of the frequency shifts and line broadenings of the lattice modes.

II. APPARATUS AND EXPERIMENTS

The single crystal used throughout the experiments is the specimen II described earlier.[1] It is 99% deuterated with dimensions (1.0×2.5×2.6 cm) and mosaic spread of about 0.3°. The single crystal was aligned with its $(1\bar{1}0)$ plane in the scattering plane. It was kept in a conduction-type cryostat. The crystal was glued to an aluminum mount in good thermal contact with, and enclosed in, a thin aluminum cassette surrounded by two radiation shields within the cryostat.

The temperature of the specimen was measured by a copper-constantan thermocouple attached to the mount, 1 cm distant from the specimen. The temperature was calibrated with an ice junction accurate to within ±0.1 °C. The calibration was checked with the boiling point of liquid nitrogen, the vapor-pressure point of CO_2, and the boiling point of water at atmospheric pressure. The agreement is always better than ±1 °C.

The temperatures during the experiments were controlled in two different ways: by adjusting the current through the heater in the range from 80 to 200 °K; and by precooling the coolant with dry ice in the range from 200 to 300 °K. The heater was

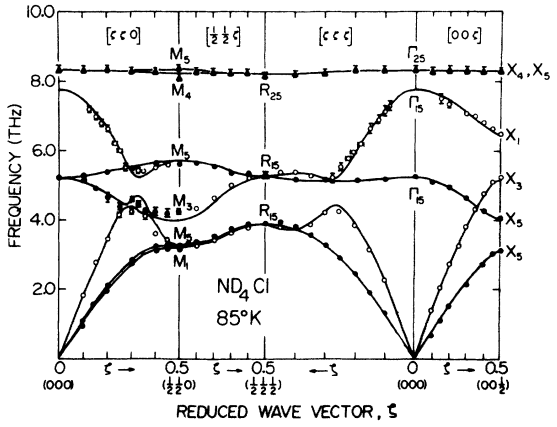

FIG. 1. Dispersion curves for ND_4Cl at 85 °K with experimental measurements of Teh and Brockhouse (Ref. 1). The reduced wave vector $\vec{\zeta} = a\vec{q}/2\pi$. The solid lines are the calculated curves for the shell model.[5] Group-theoretical notations are assigned to the modes at the zone center and the zone boundaries.

attached to the inner radiation shield. The coolant was prepared from a mixture of antifreeze, water, and acetone and was placed in the thermal reser-

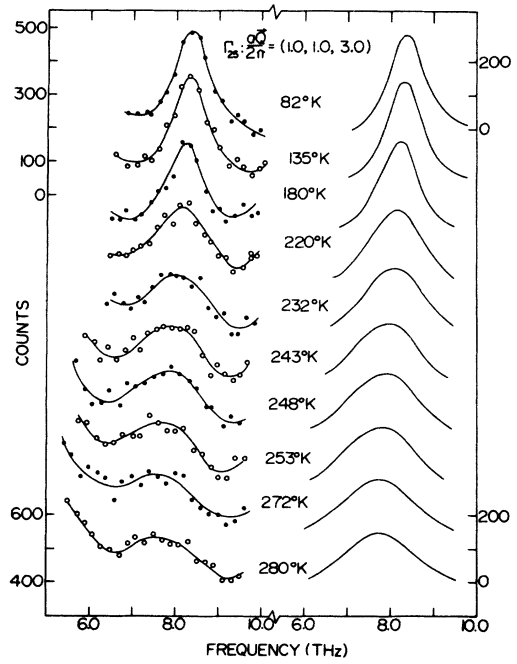

FIG. 2. Left, observed neutron groups for the librational mode Γ_{25} measured at (1, 1, 3) at various temperatures; right, the real neutron groups after correction for background counts. The two scales of counts are shown for the first and last neutron groups. Other groups are plotted with the same scale, but are displaced apart for clarity of display.

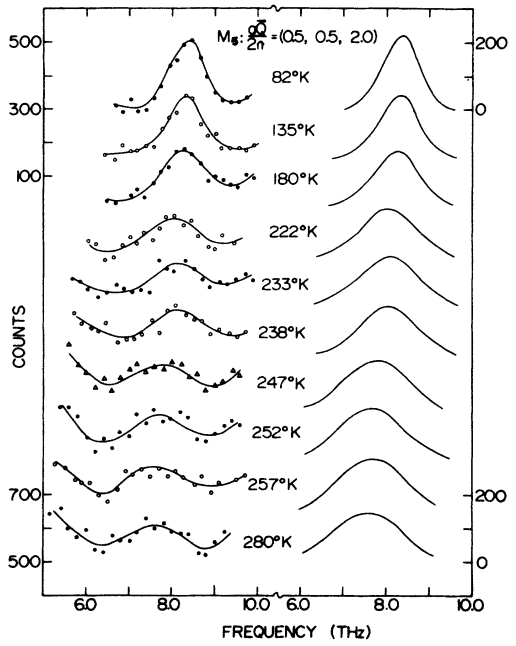

FIG. 3. Neutron groups for the librational mode M_5 measured at (0.5, 0.5, 2) at various temperatures (see Fig. 2 for further description).

voir of the cryostat. Each measurement was taken after thermal equilibrium was reached at a new temperature. The stability of the temperature was displayed on a chart recorder and was stable to within ± 0.1 °C. However there was a drift in temperature in the range from 200 to 300 °K of about 1 °K during a phonon scan (average ~ 4 h) because of the rise in temperature of the coolant.

The experiments were carried out on the McMaster triple-axis crystal spectrometer[13] at the NRU reactor of the Chalk River Nuclear Laboratories. The well-known constant-$\vec{Q}$ technique as described elsewhere[14] was employed throughout the experiments.

III. FREQUENCIES AND WIDTHS OF LATTICE MODES

The various lattice modes to be studied below were labeled with group-theoretical notations described in the previous papers.[1,2,5] The experimental and calculated dispersion curves for ND_4Cl at 85 °K reported in the above papers are reproduced in Fig. 1 for convenience of reference and identification.

The neutron groups for the librational modes Γ_{25}, M_5, and R_{25} measured at the reduced momentum transfer $a\vec{Q}/2\pi = (1, 1, 3)$, (0.5, 0.5, 2), and (2.5, 2.5, 3.5) are shown at the left-hand side of Figs. 2, 3, and 4, respectively. The intensities are normalized to a constant number of incident neutrons. These neutron groups sit on a sloping background, especially at the higher temperatures,

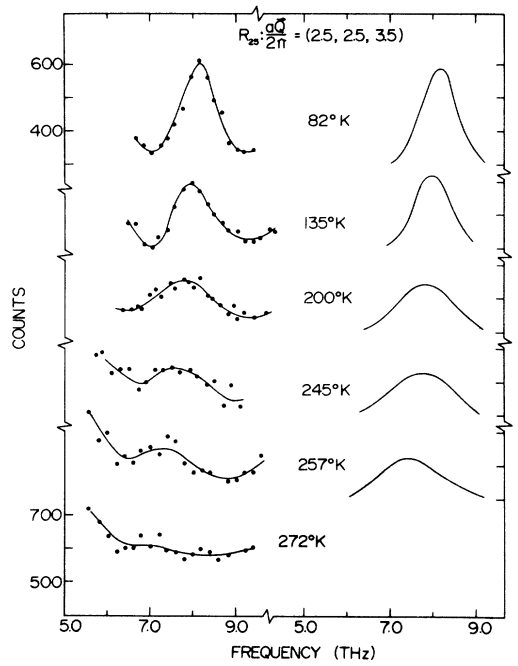

FIG. 4. Neutron groups for the librational mode R_{25} measured at (2.5, 2.5, 3.5) at various temperatures (see Fig. 2 for further description).

because of the presence of lower-frequency translational modes. This interference by the translational mode gets worse as the temperature is increased, where the groups become broader in width and are shifted towards lower frequencies. On the high-frequency side, a contaminant wavelength present in the "monochromatic" beam was always picked up by the analyzer at 10.8 THz with incident frequency of 15.0 THz. In addition, the sensitivity of the copper (200) analyzer varies because of the long frequency scan for each neutron group. Thus correction of the measured intensities is necessary. The correction was done by comparing the intensities of the neutron groups with reference to the expected theoretical value. For our experiments, in which the magnitudes of the wave vector of the incident neutron (k_0) and of the momentum transfer ($\hbar\vec{Q}$) were kept fixed, we have the following simple expression:

$$\text{Intensity} \propto (k'/\nu_s)(\langle n_s\rangle + 1)e^{-2W(\vec{Q},T)}, \qquad (1)$$

where k' is the magnitude of the wave vector of the scattered neutron, ν_s and $\langle n_s\rangle$ are, respectively, the frequency and Bose-Einstein population for the normal mode s, and $e^{-2W(\vec{Q},T)}$ is the Debye-Waller factor.

In making the correction, interpolated values[15,16] for the Debye-Waller factor were used. An appropriate sloping background can then be drawn for each neutron group (belonging to the same normal mode) by reference to the calculated intensity normalized with respect to the group measured at 82°K. In other words, the background was sketched in such a way as to seem "sensible" and to give the expected integrated intensity. An estimate of the true shape of each neutron group is then obtained by subtracting the sloping background from the observed intensity of the neutron group, and is shown on the right-hand side of each figure. The frequency for each mode is taken to be the center position of the corrected neutron group.

The instrumental width for each mode is calculated, following Cooper and Nathans,[17] using the planar approximation, good since all the groups being studied are for zone-boundary modes (and since the librational branches are practically flat throughout the whole zone). The observed width of the neutron group is defined as the full width at half-maximum (FWHM) of the corrected group, and is taken to be equal to the root-mean-square sum of the instrumental and phonon widths. The final values for the phonon widths (including some of the translational modes to be described later) are listed in Table III.

The neutron groups for the librational modes measured at momentum transfers (2, 2, 0.5) and (1, 1, 3.5) are given in Fig. 5. These are identified as X_5 modes in the notation given by Cowley.[2] The structure factor[1] for the mode X_4 was calcu-

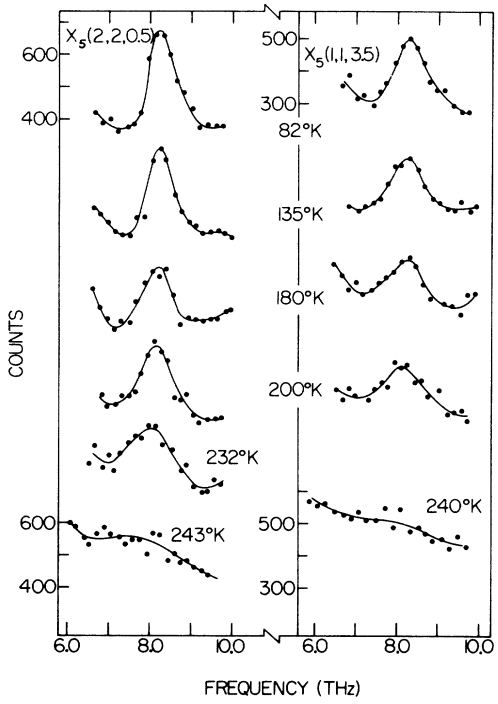

FIG. 5. Neutron groups for the librational modes measured at (2, 2, 0.5) and (1, 1, 3.5).

TABLE I. Temperature dependence of the frequencies (in units of THz) for some of the librational modes at the high-symmetry points in the Brillouin zone for ND_4Cl.

T (°K)	Γ_{25} (1.0, 1.0, 3.0)	M_5 (0.5, 0.5, 2.0)	R_{25} (2.5, 2.5, 3.5)	X_5 (1.0, 1.0, 3.5)	X_4 (2.0, 2.0, 0.5)
82 ±1	8.38 ±0.07	8.34 ±0.10	8.12 ±0.07	8.30 ±0.08	8.26 ±0.08
135 ±1	8.30 ±0.09	8.28 ±0.10	7.98 ±0.10	8.24 ±0.10	8.20 ±0.08
180 ±1	8.16 ±0.10	8.22 ±0.10	•••	8.18 ±0.10	8.16 ±0.10
200 ±1	8.15 ±0.10[a]	•••	7.82 ±0.10	8.15 ±0.10	8.10 ±0.10
221 ±2	8.10 ±0.11	8.08 ±0.12	•••	•••	•••
232 ±2	8.08 ±0.12	8.06 ±0.15	•••	•••	8.00 ±0.11
239 ±2	•••	8.04 ±0.15	•••	•••	•••
243 ± 2	7.90 ±0.14	•••	•••	•••	•••
247 ±2	7.82 ±0.14	7.76 ±0.15	7.70 ±0.12	•••	•••
253 ±1	7.76 ±0.15	7.70 ±0.15	•••	•••	•••
257 ±2	•••	7.64 ±0.15	7.50 ±0.15	•••	•••
272 ±2	7.74 ±0.15	•••	•••	•••	•••
280 ±2	7.72 ±0.15	7.56 ±0.15	•••	•••	•••

[a] Measured at $a\vec{Q}/2\pi = (3.0, 3.0, 2.0)$.

lated and found to be zero at (2, 2, 0.5) and (1, 1, 3.5). The structure factor for the mode X_5 at these two positions turned out to be large enough for the neutron groups to be observed. The librational mode M_5 (0.5, 0.5, 2) mentioned earlier is similarly identified.

Table I lists the frequencies for all the librational modes measured at the high-symmetry points at various temperatures. As shown in Fig. 4, the neutron groups for the R_{25} mode became too broad to be measured at temperatures above T_λ. This happened also for the modes X_5 (2, 2, 0.5) and X_5 (1, 1, 3.5), for which the broadening prohibited measurement beyond 232 °K.

Some of the neutron groups for the translational modes are given in Figs. 6, 7, and 8. Phonon widths for the mode M_5 (2.5, 2.5, 0) only were analyzed, since the neutron groups for the others either show little change with temperature—M_5 (2.5, 2.5, 1)—or are interfered with by another neutron group as a result of the behavior of the one-phonon

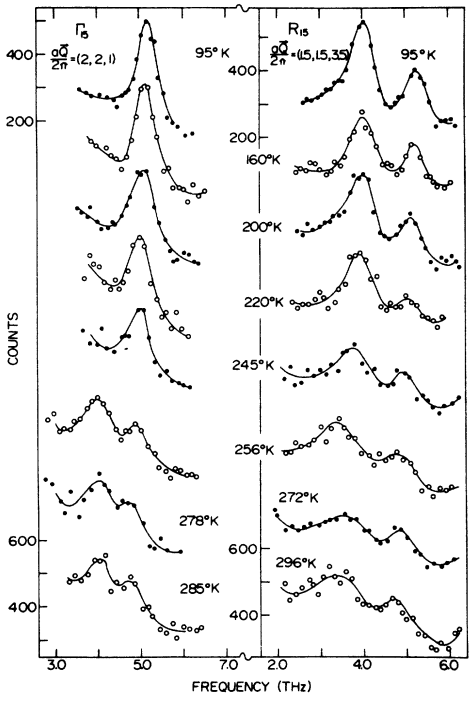

FIG. 6. Neutron groups for the translational modes Γ_{15} and R_{15} measured at (2, 2, 1) and (1.5, 1.5, 3.5), respectively. For the Γ_{15} mode, the spurious peak observed at about 4.0 THz arises from higher-order elastic scattering from the specimen.

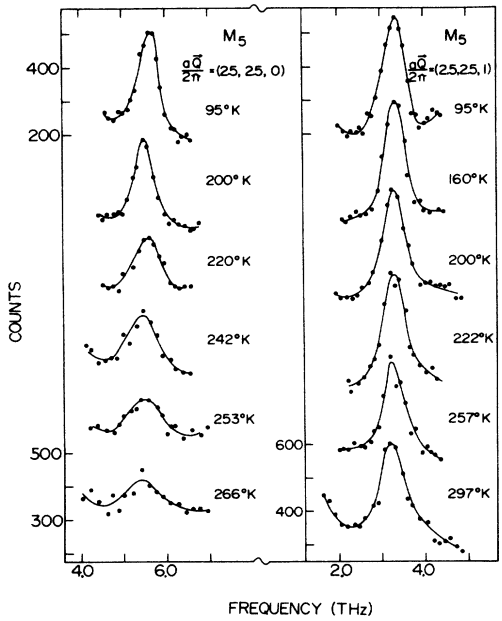

FIG. 7. Neutron groups for the two translational modes M_5 measured at (2.5, 2.5, 0) and (2.5, 2.5, 1).

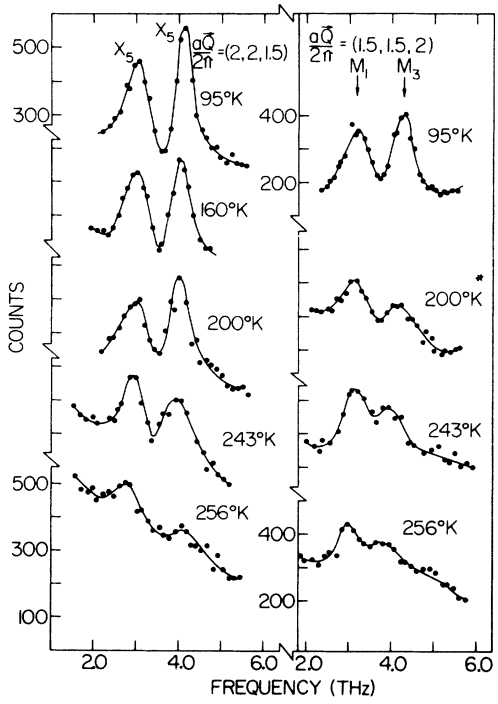

FIG. 8. Neutron groups for the various translational modes X_5, M_1 and M_3 measured at (2, 2, 1.5) and (1.5, 1.5, 2), respectively. The modes M_1 and M_3 at 200 °K were measured at (−0.5, −0.5, 3).

structure factor.

Table II lists, except for the modes X_1, X_3, and Γ_{15}(LO), the temperature dependence of the frequencies for all the translational modes at the high-symmetry points. The modes X_1 and X_3 were almost impossible to measure except at liquid-nitrogen temperature. The main reason is that these two modes are purely longitudinal and have unfavorable structure factors for almost all momentum transfers in that the two neutrons groups, being broad in width and relatively weak in intensity, are only separated by 1.25 THz. At temperatures higher than liquid-nitrogen temperature, extraneous background and mode broadening make them just too difficult to measure.

The mode Γ_{15}(LO) could not be measured, partly because of low structure factors, partly because it was always interfered with by the neutron groups of the librational modes.[1]

The frequencies are plotted as functions of temperature in Figs. 9 and 10; the widths of selected modes are plotted in Fig. 11 and listed in Table III. (The group-theoretical notation of the ordered phase is used.) Both frequencies and widths are assumed to vary continuously with temperature with maximum changes in the vicinity of T_λ for some of the modes. The relative errors in the changes of frequency and width as functions of temperature will probably be smaller than the maximum possible errors assigned to each mode since the measurements were carried out consecutively under conditions identical except for temperature. However, the maximum possible errors are shown in the figure. The dashed lines in Fig. 10 drawn by hand through the various modes should thus be quite reliable. From Fig. 11, it can be seen that

TABLE II. Temperature dependence of the frequencies (in units of THz) for some of the translational modes at the high-symmetry points in the Brillouin zone for ND_4Cl.

T (°K)	Γ_{15} (2.0, 2.0, 1.0)	R_{15} (1.5, 1.5, 3.5)		M_5 (2.5, 2.5, 1.0)	M_5 (2.5, 2.5, 0.0)
95 ±1	5.20 ±0.05	3.96 ±0.06	5.28 ±0.08	3.32 ±0.04	5.60 ±0.05
160 ±1	5.10 ±0.06	3.96 ±0.06	5.20 ±0.08	3.32 ±0.04	•••
200 ±1	5.04 ±0.05	3.95 ±0.06	5.16 ±0.08	3.30 ±0.04	5.52 ±0.05
220 ±2	5.00 ±0.06	3.88 ±0.07	5.12 ±0.10	3.30 ±0.04	5.52 ±0.06
244 ±2	4.92 ±0.06	3.75 ±0.08	4.98 ±0.10	•••	5.45 ±0.06
253 ±1	•••	•••	•••	•••	5.44 ±0.07
256 ±2	4.90 ±0.10	3.44 ±0.08	4.86 ±0.10	3.26 ±0.05	•••
266 ±2	•••	•••	•••	•••	5.40 ±0.10
272 ±2	•••	3.42 ±0.10	4.84 ±0.12	•••	•••
278 ±2	4.80 ±0.15	•••	•••	•••	•••
285 ±3	4.80 ±0.15	•••	•••	•••	5.34 ±0.12
297 ±2	•••	3.40 ±0.15	4.76 ±0.12	3.24 ±0.05	•••

T (°K)	X_5 (2.0, 2.0, 1.5)		M_1 (1.5, 1.5, 2.0)	M_3 (1.5, 1.5, 2.0)
95 ±1	3.06 ±0.05	4.12 ±0.04	3.15 ±0.06	4.28 ±0.05
160 ±1	2.98 ±0.05	4.04 ±0.05	•••	•••
200 ±2	2.94 ±0.05	4.02 ±0.04	3.10 ±0.06[a]	4.20 ±0.09[a]
243 ±1	2.90 ±0.06	4.00 ±0.09	3.08 ±0.07	4.00 ±0.10
256 ±2	2.66 ±0.12	•••	2.95 ±0.10	•••

[a] Measured at $a\vec{Q}/2\pi$ = (−0.5, −0.5, 3.0).

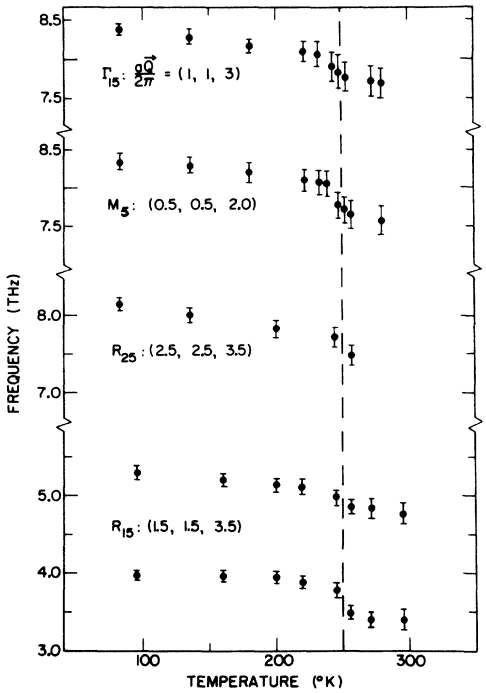

FIG. 9. Frequencies for some of the librational and translational modes as functions of temperature.

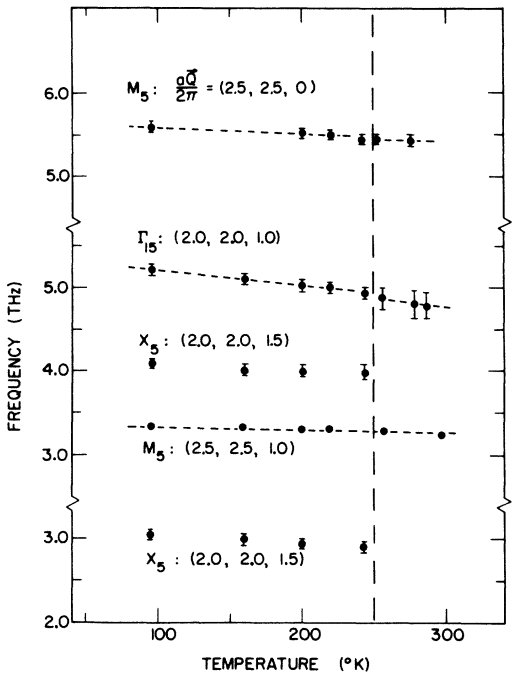

FIG. 10. Frequencies for some of the translational modes as functions of temperature.

the widths increase rapidly beyond 200 °K and get very large at temperatures above T_λ; thus the lifetimes become relatively short.

Among the translational modes, the two triply degenerate R_{15} (1.5, 1.5, 3.5) modes were found to behave similarly in frequency to the librational modes, i.e., to show an abrupt change through the transition as can be seen from Fig. 9. Other modes, such as the two X_5 modes and the M_1 and M_3 modes shown in Fig. 8, might have similar behavior, but the neutron groups become too broad to permit assignment of values before T_λ is reached. The rest of the translational modes, Γ_{15} and the two M_5 modes, differ in character from the librational modes as shown in Fig. 10. The frequencies of these modes seem to be smooth functions of temperature within the experimental errors.

TABLE III. Temperature dependence of the widths (in units of THz) for some of the librational and translational modes in ND_4Cl. The errors are indicative only.

	Γ_{25} (1.0, 1.0, 3.0) (ν = 8.38 at 82 °K)		M_5 (0.5, 0.5, 2.0) (ν = 8.34 at 82 °K)		R_{25} (2.5, 2.5, 3.5) (ν = 8.12 at 82 °K)		M_5 (2.5, 2.5, 0.0) (ν = 5.60 at 95 °K)	
T (°K)	Obs.	Real	Obs.	Real	Obs.	Real	Obs.	Real
82 ± 1	0.96 ± 0.10	0.24 ± 0.53	1.00 ± 0.10	0.37 ± 0.36	0.94 ± 0.09	0.0 ± 0.4	...	...
95 ± 1	...	...	...	...	...	...	0.56 ± 0.06	0.10 ± 0.45
135 ± 1	0.98 ± 0.10	0.31 ± 0.42	1.10 ± 0.10	0.58 ± 0.29	1.00 ± 0.12	0.31 ± 0.40	...	...
180 ± 1	1.04 ± 0.12	0.44 ± 0.33	1.32 ± 0.19	0.92 ± 0.28	...	...	...	...
200 ± 1	...	...	...	...	1.50 ± 0.18	1.15 ± 0.27	0.70 ± 0.07	0.43 ± 0.15
221 ± 2	1.40 ± 0.20	1.04 ± 0.21	1.56 ± 0.24	1.25 ± 0.34	...	...	0.80 ± 0.08	0.58 ± 0.14
232 ± 2	1.56 ± 0.23	1.27 ± 0.22	1.64 ± 0.31	1.33 ± 0.38	...	...	...	...
238 ± 2	...	...	1.68 ± 0.32	1.35 ± 0.40	...	...	...	...
243 ± 2	1.66 ± 0.24	1.36 ± 0.21	...	...	...	...	0.96 ± 0.11	0.78 ± 0.16
247 ± 2	1.72 ± 0.26	1.42 ± 0.23	1.80 ± 0.32	1.52 ± 0.41	1.60 ± 0.26	1.27 ± 0.30	...	...
253 ± 2	1.76 ± 0.31	1.47 ± 0.23	1.86 ± 0.37	1.59 ± 0.41	...	...	1.16 ± 0.14	1.02 ± 0.18
257 ± 2	...	...	1.90 ± 0.38	1.63 ± 0.43	1.68 ± 0.33	1.37 ± 0.40	...	...
266 ± 2	...	...	...	...	...	...	1.32 ± 0.20	1.19 ± 0.23
277 ± 2	1.80 ± 0.36	1.52 ± 0.26	...	...	...	...	...	...
280 ± 2	1.84 ± 0.37	1.57 ± 0.30	1.96 ± 0.39	1.71 ± 0.44	...	...	...	...

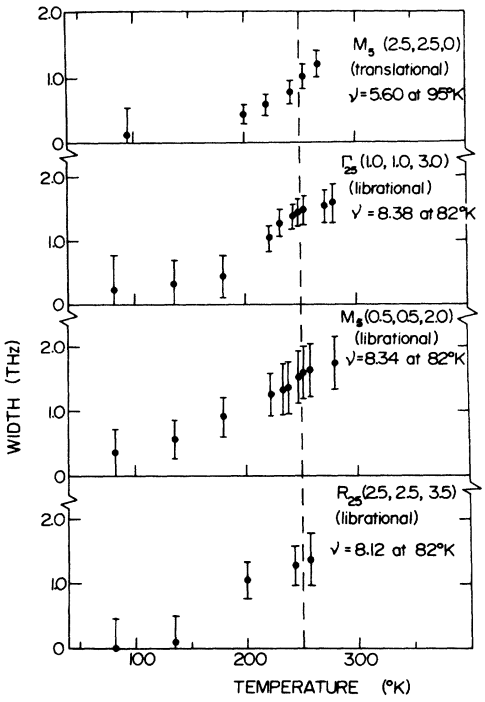

FIG. 11. Natural widths for some of the libration and translational modes as functions of temperature.

IV. DYNAMICS OF ORDER-DISORDER PHASE TRANSITION

The order-disorder phase transition in ND_4Cl manifests itself in the values for the frequencies and widths of the lattice modes presented in Sec. III. A rough picture of the dynamics of the phase transition for NH_4Cl is as follows:

The reorientation of the NH_4^+ ion is presumably thermally activated over a hindering potential barrier V produced by the eight Cl^- ions. The temperature dependence of the average reorientation frequency ν_R may therefore be written as[18]

$$\nu_R = \nu_0 e^{-E/k_B T}, \tag{2}$$

where k_B is the Boltzmann constant and E the activation energy, above the zero-point energy of libration, required for reorientation. (The zero-point energy is $E_0 = \frac{3}{2}h\nu$, with $\nu \simeq 11.7$ THz.) The values of ν_0 and E were obtained by fitting the values of ν_R to the experimental data[18] of the spin-lattice relaxation time and are given as follows:

$$E = 3.27 \times 10^{-13} \text{ erg} \quad \text{or} \quad 4700 \text{ cal/mole},$$

$$\nu_0 = 38.5 \text{ THz}.$$

The barrier height ($V = E_0 + E$) is equal to 6400 cal/mole in the ordered phase. The value for the same quantity obtained by Gutowsky *et al.*[19] is 6410 cal/mole. Thus the reorientation frequency ν_R varies from $\sim 10^3$ Hz at 90 °K to $\sim 10^{11}$ Hz at 300 °K. At all temperatures below 300 °K the flipping frequency is much less than the frequencies of the lattice vibrations seen in these experiments.

We come back to the results given in Sec. III. The functions $\nu(T)$ for the translational modes M_5, Γ_{15}, and M_5 shown in Fig. 10 are linear within the experimental accuracy. The motions of the ions involved in these modes apparently are not much affected by the order-disorder change. In particular the frequency and width of the mode M_5 (2.5, 2.5, 1) as shown in Figs. 7 and 10 were almost independent of temperature.

In general, the frequency shifts depend mainly on the thermal expansion of the unit cell and the intrinsic anharmonicity (e.g., phonon-phonon interaction). In the present case there may be, in addition, lowering of the frequencies because of the disordering process itself.

In the first place, we look at the temperature dependence of the volume of the unit cell of ND_4Cl. This is given in Fig. 15 of the Appendix. The abrupt change in volume at T_λ is very pronounced. This leads one to conjecture that the anomalous thermal expansion near T_λ induced by the transition might be responsible for the abrupt changes in the phonon frequencies (Fig. 9), in that the increases in the interatomic distances result in decreases of the force constants. This can be checked by plotting the phonon frequencies as functions of the volume of the unit cell.

Figure 12 shows the volume dependence of the frequencies for the librational modes $\Gamma_{25}(1, 1, 3)$ and $M_5(0.5, 0.5, 2.0)$ and the two translational modes $R_{15}(1.5, 1.5, 3.5)$. The anomalous change in frequency at T_λ is still quite pronounced for the mode M_5 and the lower-frequency R_{15} mode. It is reasonable to assume that the frequency shift caused

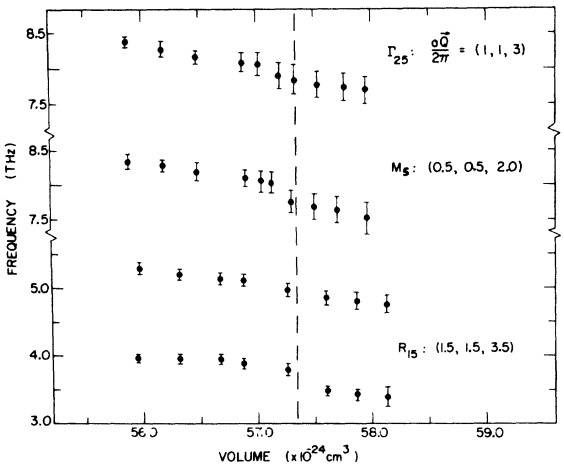

FIG. 12. Frequencies for some of the librational and translational modes as functions of the volume of the unit cell.

by the intrinsic anharmonicity is a smooth function of volume. Thus the remaining change in frequency at T_λ of Fig. 12 can be attributed to the disordering process.

It is interesting to note that, among the translational modes, the two which behave anomalously in frequency—the triply degenerate modes R_{15}—show changes in symmetry through the transition. From group-theoretical analysis,[2,20] these two modes involve the motion of both the Cl^- and ND_4^+ ions in the ordered (lower-symmetry) phase, whereas in the disordered (higher-symmetry) phase, the motion is decoupled into the modes R_{15} and R_{25} such that the lighter ND_4^+ ions only are involved in the R_{15} mode with higher frequency, and the heavier Cl^- ions in the R_{25} mode with lower frequency. (It should be noted, however, that the two doubly degenerate M_5 and the two doubly degenerate X_5 modes also involve change in symmetry at the transition. The M_5 modes do not show much effect from the transition. It is not possible to follow the X_5 modes through the transition because of extreme broadening).

On the other hand, the M_1 mode also seems probably to have an abrupt change in frequency at T_λ as seen from Fig. 8. Although this mode is not affected by symmetry, the eigenvector as obtained from the shell-model calculation[5] of Fig. 1 indicates that there is about 2% mixing-in of librational motion. Other translational modes which show mixing with the librational motions are the higher-frequency M_5 and the two X_5 modes. All of these show considerable broadening indicating short lifetimes. For those modes which are purely translational, such as Γ_{15}(TO), the two R_{15} modes, and the lower M_5 mode, the neutron groups are well defined at temperatures up to 300°K.

Another point worth noticing is the large broadening of the librational modes at X and R which occurred at temperatures lower than T_λ (Figs. 4 and 5). This might be related to the fact that the two lowest activation energies for the reorientation of the ND_4^+ ions are those associated with rotations about the fourfold and threefold axes,[19] though the frequencies of reorientation at these temperatures are less than 1% of the frequencies of libration.

V. ELASTIC-CONSTANT DETERMINATION

The high-frequency phonons (or sound waves) detected by neutron scattering techniques normally propagate in the zero-sound region ($\omega\tau \gg 1$), where ω and τ are, respectively, the angular frequency and lifetime of the phonon. On the other hand, the low-frequency sound waves as detected by ultrasonic techniques lie in the first-sound region ($\omega\tau \ll 1$). As pointed out by Cowley,[21] the elastic constants obtained in anharmonic crystals by these two different techniques are expected to differ. Measurements[22] on KBr and $SrTiO_3$ have demonstrated this difference. In the present case, the values of the adiabatic elastic constants c_{44} and c_{11}, presumably in the zero-sound region, were determined by measuring the limiting slopes of the [001]TA and [001]LA branches in the $(1\bar{1}0)$ plane, respectively.

The slopes were determined by measuring the phonon frequencies at two positive wave vectors with phonon creation and at two negative wave vectors with phonon annihilation covering as much as possible the linear region of the dispersion curves. The instrumental resolution was arranged such that the horizontal divergences of both the incident and scattered beam were $\frac{3}{4}°$, and the vertical divergences 2°. The observed frequencies given in Table IV were not corrected quantitatively for resolution and dispersion effects; the possible errors in the calculated elastic constants coming from these effects will be discussed later. The elastic constants with estimated errors were determined by least-squares fitting to the various sets of observed frequencies.

The values of the elastic constants thus obtained for ND_4Cl were compared with those obtained by ultrasonic techniques[11] for NH_4Cl. As shown in Fig. 13, the temperature dependence of the elastic constants for ND_4Cl is qualitatively similar to that for NH_4Cl, but quantitatively the difference is quite significant. In view of the fact of the loose colli-

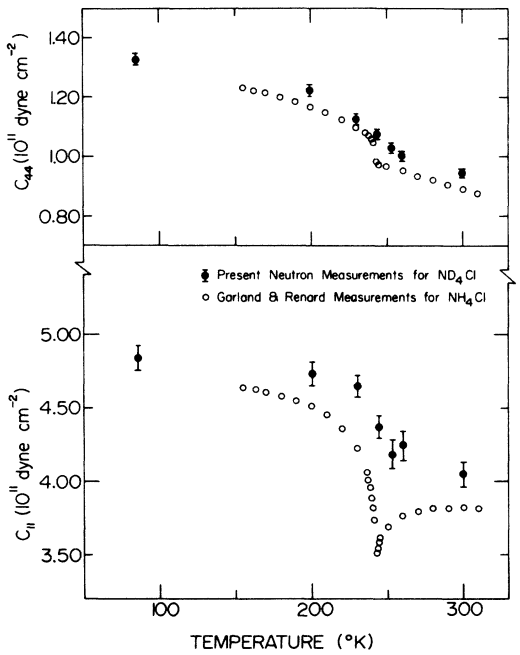

FIG. 13. Temperature dependence for the elastic constants of ND_4Cl and NH_4Cl, as measured by neutron scattering and ultrasonic techniques, respectively. The values obtained by neutron scattering are not corrected for resolution and dispersion effects.

TABLE IV. Frequencies (in units of THz) of the acoustic phonons along the [00ζ] LA and TA branches and the elastic constants C_{11} and C_{44} (in units of 10^{11} dyn cm^{-2}) as calculated from the limiting slopes of the LA and TA branches, respectively. a is the lattice parameter in units of 10^{-8} cm.

			[00ζ] LA			
T (°K)	0.10	0.15	−0.10	−0.15	a	c_{11}
85	1.42 ± 0.03[a]	2.06 ± 0.03	−1.42 ± 0.03[a]	−2.08 ± 0.03	3.824	4.87 ± 0.08
200	1.41 ± 0.03	2.05 ± 0.03	−1.41 ± 0.03	−2.05 ± 0.03	3.840	4.77 ± 0.08
230	1.41 ± 0.03	2.03 ± 0.03	−1.39 ± 0.03	−2.03 ± 0.03	3.848	4.67 ± 0.08
244	1.38 ± 0.03	1.95 ± 0.03	−1.37 ± 0.03	−1.97 ± 0.03	3.853	4.40 ± 0.08
253	1.32 ± 0.04	1.92 ± 0.04	−1.34 ± 0.04	−1.94 ± 0.04	3.860	4.21 ± 0.10
260	1.33 ± 0.04	1.97 ± 0.04	−1.32 ± 0.04	−1.94 ± 0.04	3.865	4.27 ± 0.10
300	1.32 ± 0.04	1.90 ± 0.03	−1.30 ± 0.03	−1.91 ± 0.04	3.874	4.07 ± 0.08
			[00ζ] TA			
T (°K)	0.15	0.20	−0.15	−0.20	a	c_{44}
85	1.11 ± 0.02	1.46 ± 0.02	−1.09 ± 0.02	−1.45 ± 0.02	3.824	1.30 ± 0.02
200	1.07 ± 0.02	1.40 ± 0.02	−1.05 ± 0.02	−1.39 ± 0.02	3.840	1.19 ± 0.02
230	1.01 ± 0.02	1.34 ± 0.02	−1.02 ± 0.02	−1.35 ± 0.02	3.848	1.10 ± 0.02
244	0.98 ± 0.02	1.31 ± 0.02	−0.99 ± 0.01	−1.33 ± 0.02	3.853	1.05 ± 0.02
253	0.98 ± 0.02	1.29 ± 0.02	−0.97 ± 0.02	−1.28 ± 0.02	3.860	1.00 ± 0.02
260	0.96 ± 0.02	1.27 ± 0.02	−0.96 ± 0.02	−1.27 ± 0.02	3.865	0.97 ± 0.02
300	0.94 ± 0.02	1.24 ± 0.02	−0.92 ± 0.02	−1.23 ± 0.02	3.874	0.92 ± 0.02

[a] The + and − signs for the values of the phonon frequency referred to phonon creation and annihilation, respectively. The frequencies were not corrected for resolution but the elastic constants were.

mation in the present measurement, the possible errors which might have arisen from the instrumental resolution were estimated by calculating the angular dependence of the sound velocities in the (001) and (1$\bar{1}$0) planes using the "Cristoffel equation"[23] and then averaging over the resolution. The ratios of the three elastic constants vary considerably over the range of temperature covered by the experiments. The resolution effect is therefore temperature dependent. The effect came largely from the vertical divergence of the collimator system (~ ± 1°) which produces an uncertainty in the direction of propagation of the sound waves of up to ±12° away from the nominal symmetry direction. Because the wave vectors are in symmetry directions, the possible error in c_{11} turns out to be no more than 1.5% and that in c_{44} no more than 4%. But the assigned errors for the measured frequencies leads to an unexpected error for c_{44} of less than 2%, as can be seen from Fig. 13; thus a correction to c_{44} is necessary. The sign for correction can be determined from the angular dependence of the calculated sound velocities in the (100) and (1$\bar{1}$0) planes. On averaging over the directions of propagation of the sound waves within the solid angle defined by the resolution, corrections of −2.5% for c_{44} and +0.75% for c_{11} are obtained. The values for c_{11} and c_{44} after correction are given in Table IV. The difference between the elastic constants

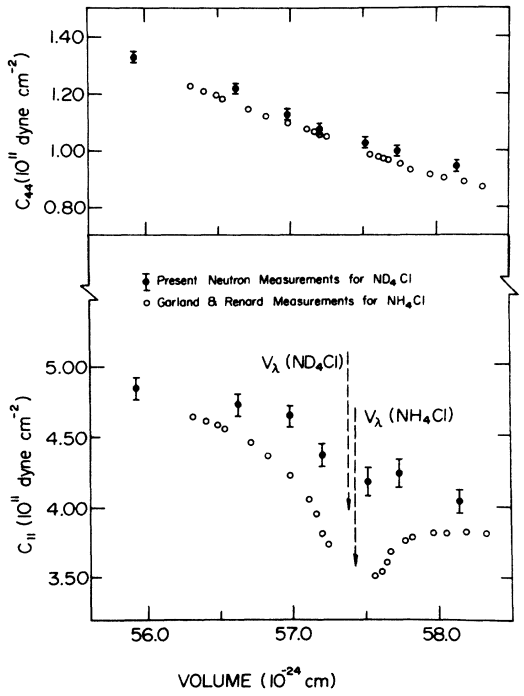

FIG. 14. Elastic constants of ND_4Cl and NH_4Cl plotted as functions of the volume of the unit cell. The volume at the corresponding transition temperature is denoted V_λ. The values obtained by neutron scattering are not corrected for resolution and dispersion effects.

TABLE V. Lattice constants of ND_4Cl.

T (°K)	Lattice constant obtained from various scattering planes (Å) (300)	(311)	(222)	Average value (Å)
296	3.8725	3.8741	3.8735	3.8734
275	3.8681	3.8690	3.8685	3.8686
253	3.8557	3.8581	3.8603	3.8581
240	3.8510	3.8516	3.8533	3.8520
197	3.8392	3.8400	3.8400	3.8397
90	3.8242	3.8244	3.8242	3.8243

c_{11} for ND_4Cl (measured with neutrons) and for NH_4Cl (measured with ultrasonics) is thus significant.

The uncorrected values of the elastic constants are plotted as functions of the volume of the unit cell in Fig. 14. It is interesting to note that the values of c_{44} for both ND_4Cl and NH_4Cl lie, within the experimental accuracy, on the same, almost linear, curve. For c_{11}, on the other hand, the curves for the two materials are significantly different. The difference might possibly be caused by the deuteration, because the zero-point motions differ in the deuterated and nondeuterated materials, but this is considered unlikely. It is much more likely that the difference arises from an effect analogous to the difference between first sound and zero sound: For low enough frequencies the degree of order would be expected to be in equilibrium locally, as the wave propagates. For high frequencies, in particular for frequencies higher than the flipping frequency of the tetrahedra, the local degree of order cannot follow the wave in its alternate rarefactions and compressions. As has already been discussed, the flipping frequency at temperatures in the vicinity of T_λ is indeed in between the ultrasonic frequency and the effective neutron frequency. If this explanation of the phenomenon of Fig. 14 is correct, it implies thermodynamically that T_λ changes when the specimen is subjected to the volume-changing distortion described by c_{11} but changes much less when subjected to the shear described by c_{44}. The transition temperature does increase considerably with applied hydrostatic pressure,[11] so this result is quite likely.

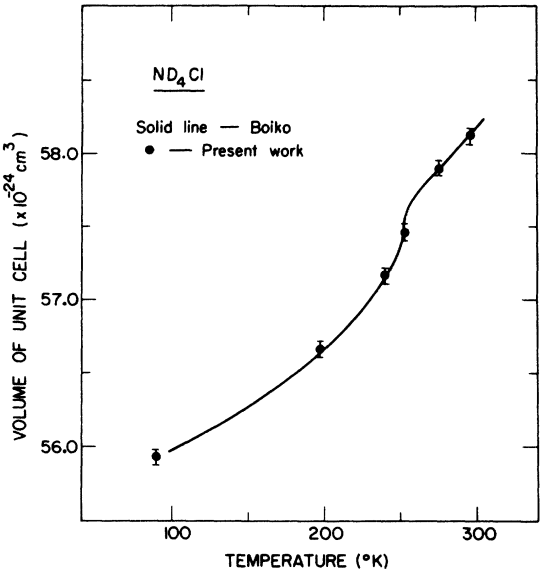

FIG. 15. Temperature dependence of the volume of the unit cell for ND_4Cl as measured using x rays by Boiko and in these experiments.

ACKNOWLEDGMENTS

The authors wish to express their appreciation to the National Research Council of Canada for financial support, to the staff at the Atomic Energy of Canada Ltd. at Chalk River for their cooperation, to J. D. Cooper for invaluable technical assistance, and to G. Dolling and E. R. Cowley for helpful discussions.

APPENDIX: LATTICE PARAMETER OF ND_4Cl

The method of neutron diffraction[24] is convenient for measuring the average lattice constant of large single crystals. The lattice constants of ND_4Cl were measured at six different temperatures lying between 90 and 300 °K using an incident wavelength of 2.034 Å. The results obtained are given in Table V. They are in good agreement with those reported as resulting from x-ray measurements[25] and from hydrostatic-weight measurements.[26] The volumes of the unit cell at various temperatures were calculated from the lattice constants obtained in the present experiments and from the x-ray results, and are shown in Fig. 15.

†Work supported by the National Research Council of Canada.

[1]H. C. Teh and B. N. Brockhouse, Phys. Rev. B **3**, 2733 (1971). H. C. Teh, B. N. Brockhouse, and G. A. DeWit, Phys. Lett. A **29**, 694 (1969).
[2]E. R. Cowley, Phys. Rev. B **3**, 2743 (1971).
[3]H. Jex, Phys. Lett. A **34**, 118 (1971); Solid State Commun. **9**, 2057 (1971).
[4]C. H. Kim, H. A. Rafizadeh, and S. Yip, J. Chem. Phys. **57**, 2291 (1972).
[5]H. C. Teh, Can. J. Phys. **50**, 2807 (1972).
[6]E. L. Wagner and D. F. Hornig, J. Chem. Phys. **18**, 296 (1950).
[7]N. E. Schumaker and C. W. Garland, J. Chem. Phys. **53**, 392 (1970).
[8]C. H. Perry and R. P. Lowndes, J. Chem. Phys. **51**, 3648 (1969).
[9]I. Freund and L. Kopf, Phys. Rev. Lett. **24**, 1017 (1970).
[10]C. H. Wang, Phys. Rev. Lett. **26**, 1226 (1971).
[11]C. W. Garland and R. Renard, J. Chem. Phys. **44**, 1130 (1966).
[12]H. G. Smith, J. G. Traylor, and W. Reichardt, Phys. Rev. **181**, 1218 (1969).

[13]B. N. Brockhouse, G. A. DeWit, E. D. Hallman, and J. M. Rowe, in *Neutron Inelastic Scattering Vol. II* (International Atomic Energy, Vienna, 1968), p. 259.
[14]E. C. Svensson, B. N. Brockhouse, and J. M. Rowe, Phys. Rev. **155**, 619 (1967).
[15]H. A. Levy and S. W. Peterson, Phys. Rev. **86**, 766 (1952).
[16]G. H. Goldschmidt and D. G. Hurst, Phys. Rev. **83**, 88 (1951).
[17]M. J. Cooper and R. Nathans, Acta Crystallogr. **23**, 357 (1967).
[18]Sachs and Turner, quoted by G. E. Pake, in *Solid State Physics*, edited by F. Seitz and D. Turnbull (Academic, New York, 1957) Vol. 2, p. 79.
[19]H. S. Gutowsky, G. E. Pake, and R. Bersohn, J. Chem. Phys. **22**, 643 (1954).
[20]S. H. Chen and V. Dvorak, J. Chem. Phys. **48**, 4060 (1968).
[21]R. A. Cowley, Proc. Phys. Soc. Lond. **90**, 1127 (1967).
[22]R. A. Cowley, W. J. L. Buyers, E. C. Svensson, and G. L. Paul, in *Neutron Inelastic Scattering Vol. I* (International Atomic Energy, Vienna, 1968), p. 281
[23]J. de Launay, in *Solid State Physics*, edited by F. Seitz and D. Turnbull (Academic, New York, 1957), Vol. 2, p. 265.
[24]S. C. Ng, B. N. Brockhouse, and E. D. Hallman, Mater. Res. Bull. **2**, 69 (1967).
[25]A. A. Boiko, Kristallografiya **14**, 639 (1969) [Sov. Phys.-Crystallogr. **14**, 539 (1970)].
[26]P. Nissila and J. Poyhonen, Phys. Lett. A 33, 345 (1970).